Letter

Controlling Diffraction Patterns with Metagratings

Vladislav Popov,[1,*] Fabrice Boust,[1,2,†] and Shah Nawaz Burokur[3,‡]

[1] *SONDRA, CentraleSupélec, Université Paris-Saclay, F-91190, Gif-sur-Yvette, France*
[2] *DEMR, ONERA, Université Paris-Saclay, F-91123, Palaiseau, France*
[3] *LEME, UPL, Univ Paris Nanterre, F92410, Ville d'Avray, France*

(Received 23 March 2018; revised manuscript received 18 May 2018; published 24 July 2018)

In this study, we elaborate on the recent concept of metagratings proposed in Ra'di *et al.* [Phys. Rev. Lett. 119, 067404 (2017)] for efficient manipulation of reflected waves. Essentially, a metagrating is a set of 1D arrays of polarization line currents which are engineered to cancel scattering in undesirable diffraction orders. We consider a general case of metagratings composed of N polarization electric line currents per supercell. This generalization is a necessary step to totally control diffraction patterns. We show that a metagrating having N equal to the number of plane waves scattered in the far field can be used to control the diffraction pattern. To validate the developed theoretical approach, anomalous and multichannel reflections are demonstrated with 3D full-wave simulations in the microwave regime at 10 GHz. The results are interesting for the metamaterials community as they allow one to significantly decrease the number of used elements and simplify the design of wavefront manipulation devices, which is very convenient for optical and infrared frequency ranges. Our findings may also provide a way to develop efficient tunable antennas in the microwave domain.

DOI: 10.1103/PhysRevApplied.10.011002

For a long time, the microwave community has approached a particular problem of anomalous reflection by means of reflectarray antennas [1,2]. In such antennas, a linear phase variation is created along the surface, allowing one to reflect incident waves to a desirable angle. With the development of nanofabrication technologies and metasurfaces, the concept of reflectarrays was transposed to infrared and optical frequency domains [3,4]. A metasurface is represented by a 2D dense distribution of subwavelength scatterers and a reflectarray is a particular case of a metasurface which can generally be used for various applications other than anomalous reflections. However, reflectarrays suffer from low efficiencies for angles of anomalous reflection approximately greater than 45° [5]. Extensive research in this area established a strong theoretical grounding in the form of the equivalence principle [6] for the design of wavefront manipulation devices based on the use of metasurfaces. As such, multichannel reflection with metasurfaces was demonstrated both theoretically and experimentally in Ref. [7]. Recently, a metasurface performing highly efficient anomalous reflection at a steep angle has been demonstrated in Ref. [8] on the basis of the concept of metasurfaces possessing strong spatial dispersion [5,9]. Unfortunately, a theoretical framework to design strongly spatial dispersive metasurfaces has not been developed yet, making the design of a sample time consuming (if it is possible at all) as it requires 3D full-wave simulations. In spite of advances in the field of metasurfaces, drawbacks concerning design complexity and material losses still exist, rendering implementation of high-performance devices very challenging in some frequency ranges [10].

In this study, we elaborate on the recent concept of metagratings [11] for the manipulation of reflected waves. Essentially, a metagrating is a set of 1D arrays of scatterers such as polarization line currents, separated by a distance of the order of the operating wavelength λ. Polarization line currents are used to cancel scattering in undesirable diffraction orders. Metagratings allow one to significantly decrease the number of constitutive scatterers in contrast to metasurfaces where scatterers are tightly packed in the plane. This reduction can be very attractive to reduce the fabrication complexity as well as the joule losses.

On the theoretical level, metasurface and metagrating are described differently. As a metasurface is composed of deeply subwavelength tightly packed elements, one can introduce averaged surface impedances. Meanwhile, a metagrating is treated as an array of polarization line currents separated by distances much larger than their sizes. Even though there can be many polarization line currents in a supercell, the separation between the currents remains on the order of the operating wavelength

*uladzislau.papou@centralesupelec.fr
†fabrice.boust@onera.fr
‡sburokur@parisnanterre.fr

and one would speculate by introducing average surface impedances.

It has been already shown that having just a single line current per period allows one to cancel specular reflection and perform perfect beam splitting and anomalous reflection [11–13]. In Ref. [14], the authors numerically and experimentally demonstrated the possibility of performing highly efficient broadband anomalous reflection with a Huygens metasurface having just two meta-atoms per supercell necessary for cancelling specular reflection. The same functionality was demonstrated in Ref. [11,13], where a single meta-atom per supercell and the substrate thickness were used as degrees of freedom instead of two meta-atoms per supercell. In this sense, the work in Ref. [14] is very similar to the ones on metagratings. Chalabi *et al.* also demonstrated the possibility of performing near-perfect anomalous reflection using two line currents per supercell [15], which are necessary for eliminating reflection in the zeroth and minus first diffraction orders. Recently, an implementation of a graphene-based tunable metagrating operating in the THz frequency range was suggested in [16].

In the present work, we study a general case of metagratings having N polarization line currents per supercell. This generalization is a necessary step for controlling diffraction patterns when the number of plane waves scattered in the far field is greater than three. Although the authors of Ref. [14] discussed the number of meta-atoms per supercell necessary for controlling an arbitrary number of plane waves diffracted in the far field, a clear theory for designing a N-meta-atom Huygens metasurface was not elaborated.

Gaining control over many diffraction orders can be particularly interesting for implementing tunable devices and performing multichannel reflection. Indeed, having many identical wires but being able to control polarization currents in each of them allows one to perform all possible transformations of the diffraction pattern with the same device, where the only restriction remains the device size. Moreover, metagratings can operate in a broad frequency range as usually they do not require the resonance response of meta-atoms. The broadband response of metagratings with a single and a couple of polarization currents per supercell was demonstrated in Refs. [13,15], respectively.

As a physical system, we consider a 1D periodic array of polarization electric line currents placed over a grounded dielectric substrate of thickness h and excited by an incident harmonic TE-polarized plane wave at angle θ, where $\exp[j\omega t]$ time dependence is assumed. The array has period L and consists of supercells each having N equally separated line currents by the distance $d = L/N$. The schematics of the considered system is presented in Fig. 1(a). A line current is imagined as a tightly packed row of point dipoles orientated in the same direction, see Fig. 1(b). Practically, one can realize the dipoles as the loaded rods considered in Figs. 1(c) and 1(d).

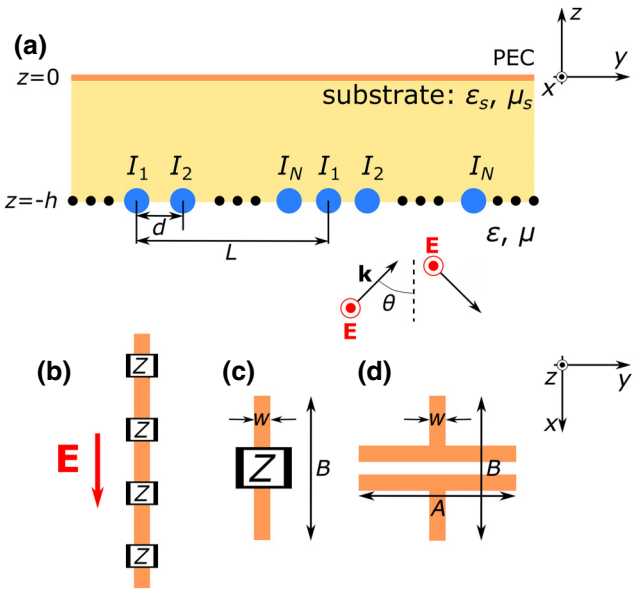

FIG. 1. (a) System under consideration: a periodic array of line currents $\mathbf{J}_{nq} = I_q \exp[-jk\sin(\theta)nL]\delta(y - y_{nq}, z + h)\mathbf{x_0}$ (blue circles) placed on a perfect electric conductor- (PEC-)backed dielectric substrate having permittivity ε_s, permeability μ_s, and thickness h. The array is excited by a plane-wave incident at angle θ with TE polarization. (b) Line current implemented as a 1D array of loaded dipoles. (c) PEC strip dipole of length B and width w loaded with lumped impedance Z. (d) PEC strip dipole loaded with printed circuit capacitance with arms of length A.

In the presence of the grounded substrate, the excitation field takes the following form:

$$E_x^{\text{exc}}(y, z \le -h) = (e^{-j\beta_0 z} + R_0^{\text{TE}} e^{j\beta_0(z+2h)}) e^{-jk\sin[\theta]y}. \quad (1)$$

Electric line currents in the array are represented as current densities $\mathbf{J}_{nq}(\mathbf{r}) = I_q \exp[-jk\sin(\theta)nL]\delta(y - y_{nq}, z + h)\boldsymbol{x_0}$, where $\delta(y, z)$ is the Dirac δ function, $y_{nq} = nL + (q-1)d$, n and q take integer values from $-\infty$ to $+\infty$ and from 1 to N, respectively. The term $\exp[-jk\sin(\theta)nL]$ represents the phase variation of the currents introduced by the incident wave. Radiation of the array of electric line currents is represented by a series of Hankel functions [17,18] of the second kind. It can be shown by means of Poisson's formula (see the Supplemental Material [19]) that the electric field of the wave radiated by the array outside the substrate can be written as

$$E_x(y, z < -h) = -\frac{k\eta}{2L} \sum_{m=-\infty}^{+\infty} \frac{\rho_m^{(I)}(1 + R_m^{\text{TE}})}{\beta_m} e^{-j\xi_m y + j\beta_m(z+h)}, \quad (2)$$

where $E_y = E_z = 0$. Corresponding magnetic fields can be found from the Maxwell equations. The series represent superpositions of plane waves having a tangential component of the wave vector equal to $\xi_m = k\sin(\theta) + 2\pi m/L$,

the longitudinal component is given by $\beta_m = \sqrt{k^2 - \xi_m^2}$ outside the substrate ($k = \omega\sqrt{\varepsilon\mu}$ and $k_s = \omega\sqrt{\varepsilon_s\mu_s}$ are, respectively, the wave numbers outside and inside the substrate). Thus, R_m^{TE} is Fresnel's reflection coefficient from the grounded substrate of a plane wave having a tangential component of the wave vector equal to ξ_m. Each current contributes to the amplitudes of the plane waves via the introduced quantity $\rho_m^{(I)}$:

$$\rho_m^{(I)} = \sum_{q=1}^{N} I_q \exp[j\,\xi_m(q-1)d]. \tag{3}$$

One can recognize in Eq. (3) a discrete Fourier transformation.

In the general case, when a plane wave illuminates a metagrating, one finds $r + l + 1$ scattered plane waves in the far field, where r and l are the largest integers satisfying the conditions $\beta_r > 0$ and $\beta_{-l} > 0$. However, we can arbitrary control all of the $r + l + 1$ plane waves if the number N of line currents in a supercell is equal to $r + l + 1$. Indeed, amplitude A_m^{TE} of the mth plane wave depends on $\rho_m^{(I)}$, which is determined by the currents I_q [see Eq. (2)]

$$A_m^{\mathrm{TE}} = -\frac{k\eta}{2L}\frac{\rho_m^{(I)}(1 + R_m^{\mathrm{TE}})e^{j\beta_m h}}{\beta_m} + \delta_{m0}R_0^{\mathrm{TE}}e^{2j\beta_0 h}, \tag{4}$$

where δ_{m0} is the Kronecker δ accounting for the incident wave reflected from the substrate. By setting all the amplitudes A_m^{TE} ($m \in [-l, r]$), one can find necessary I_q from the corresponding $\rho_m^{(I)}$, which are related via Eq. (3).

Thus, by designing currents I_q one can perform all possible transformations of the diffraction pattern, e.g., beam splitting, anomalous reflection, multichannel reflection, etc. When implementing line currents as thin perfectly conducting wires one can obtain necessary currents I_q by loading wires with suitable impedance densities Z_q. The last are found from

$$Z_q I_q = E_x^{(\mathrm{exc})}(y_{0q}, -h) - Z_{in}I_q - \sum_{p=1}^{N} Z_{qp}^{(m)} I_p, \tag{5}$$

where the right-hand side simply represents the total electric field at the location of the qth wire in the zeroth supercell [$y_{0q} = (q-1)d$, $z = -h$]. Here, we also introduce notations for the input impedance density of wires $Z_{\mathrm{in}} = k\eta H_0^{(2)}[kr_0]/4$, with $H_0^{(2)}[kr_0]$ being the Hankel function of the second kind and r_0 the radius of the wires, and for the mutual impedance densities $Z_{qp}^{(m)}$, which account for interaction between the wires and between the wires and the grounded substrate. When a wire is realized as a perfectly conducting strip of width w, the radius is $r_0 = w/4$ [18]. See the Supplemental Material [19] for the derivation of Eq. (5) and expressions of the mutual impedance densities.

Generally, currents found from Eq. (4) correspond to active and lossy loads Z_q calculated from Eq. (5). From a practical point of view, we are interested only in passive and lossless metagratings, where $\Re[Z_q] = 0$, i.e., metagratings which cannot radiate energy by themselves and do not require engineered joule losses. A metagrating should redistribute the energy of the incident wave between $r + l + 1$ diffracted in the far-field plane waves. Then, the power conservation condition when assuming a unity amplitude of the incident wave reads

$$\sum_{m=-l}^{r} \alpha_m = 1, \quad \alpha_m = |A_m^{\mathrm{TE}}|^2 \frac{\beta_m}{\beta_0}, \tag{6}$$

where α_m is the part of the incident energy going in the mth diffraction order.

In contrast to the case of metagratings having a single-line current in a supercell [11–13], when it comes to a greater number of line currents per supercell there are no exact analytical formulas for reactive load-impedance densities necessary for obtaining some diffraction pattern. To approach this problem, we develop a very simple real-valued genetic algorithm [20], which allows one to find reactive Z_q with given impedance reactivity accuracy p for a desired diffraction pattern obtained with given transformation accuracy α. The impedance reactivity accuracy is defined in accordance with the following inequality: $\sqrt{\sum_{q=1}^{N} |Re[Z_q]/Z_q|^2} < p$. A diffraction pattern is set by assigning to all α_m^0 certain values. Phases $\phi_m = \arg[A_m^{\mathrm{TE}}]$ are assumed to be unimportant and are assigned randomly. Transformation accuracy α means that one is satisfied with a transformation when the part of the incident energy going in the mth diffraction order is within the range $\alpha_m = \alpha_m^0 \pm \alpha$. Still, at each step the genetic algorithm deals with $\alpha_m > 0$ constrained by the energy conservation condition, Eq. (6).

When designing a metagrating, one should also take care of choosing parameters of the substrate. First of all, when the substrate's thickness is varied the value of the excitation field, Eq. (1), on a metagrating passes through zeros as illustrated in Fig. 2(a). Clearly, a metagrating cannot be excited when the excitation field is zero on its plane. And secondly, the reflection coefficient R_m^{TE} as a function of h has poles when m is such that $k < \xi_m$ but $k_s > \xi_m$ [Fig. 2(b)]. The poles correspond to the excitation of waveguide modes inside the substrate. Thus, assuming ε_s and μ_s of the substrate are set, one should choose the thickness: (i) corresponding to the vicinity of the maximum of the excitation field on a metagrating and (ii) $|R_m^{\mathrm{TE}}(h)| \neq \infty$.

One can realize the line currents as dense 1D arrays of loaded dipoles (separated by distance $B \ll \lambda$ and having lumped load equal to Z) as in Figs. 1(b) and 1(c). Then, the load-impedance density is simply Z/B. A capacitive load can be realized as a printed circuit capacitance as

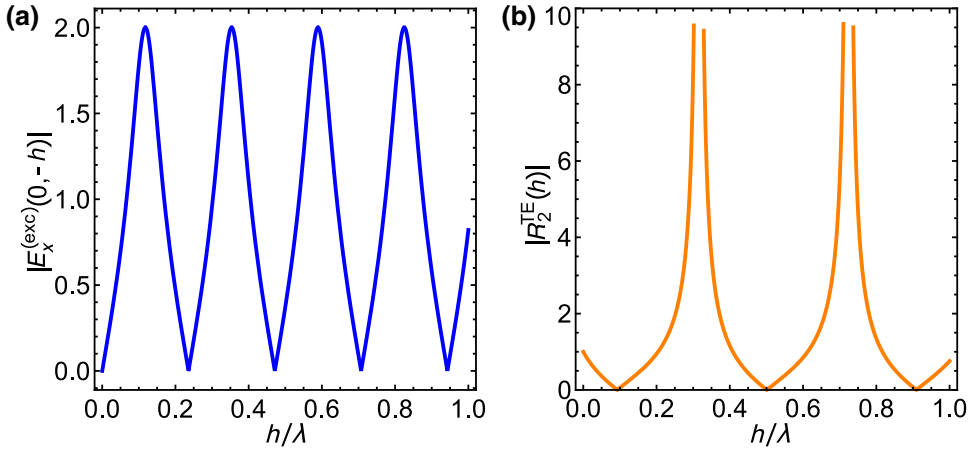

FIG. 2. (a) Dependence of the excitation field [$\theta = 0$] acting on a metagrating on the thickness of the substrate h when $\varepsilon_s = 4.5$ and $\mu_s = 1$. (b) Absolute values of the R_2^{TE} vs the thickness of the substrate when $\theta = 0$, $r = l = 1$, $N = 3$, and $L = \lambda/\sin[60^\circ]$. The rest of R_m^{TE} does not have poles under these parameters. λ is the operating vacuum wavelength.

illustrated in Fig. 1(d) for which $Z = -j\,\eta\kappa/(A\varepsilon_{\mathrm{eff}})$ (when other parameters B and w are fixed), κ is the proportionality factor, $\varepsilon_{\mathrm{eff}}$ is approximated as $(1+\varepsilon_s)/2$, and μ_s is assumed equal to 1. The proportionality factor κ was introduced in Ref. [12] for the case of a single-line current per supercell. However, it turns out that in the general case of many line currents per supercell one can successfully use the same proportionality factor for all currents, i.e., independently on q. Thus, when load-impedance densities Z_q are found from the genetic algorithm, one can easily calculate the arm lengths of necessary printed capacitors as $A_q = -\tilde{\kappa}/(\Im[Z_q](\lambda/\eta)\varepsilon_{\mathrm{eff}})$, $\tilde{\kappa} = \lambda\kappa/B$.

In order to validate the developed theoretical basis, we perform 3D full-wave simulations with COMSOL MULTIPHYSICS. We demonstrate three examples of metagratings designed to operate at 10 GHz ($\lambda \approx 30$ mm) and perform different transformations of the diffraction pattern as shown in Fig. 3. A polarization line current is implemented as a 1D array of capacitively loaded perfectly conducting strips (as is schematically shown in the top row of Fig. 3). In all examples, a normally incident plane wave is assumed, i.e., $\theta = 0$.

When performing a large-angle anomalous reflection with a metagrating, overall there are three diffraction

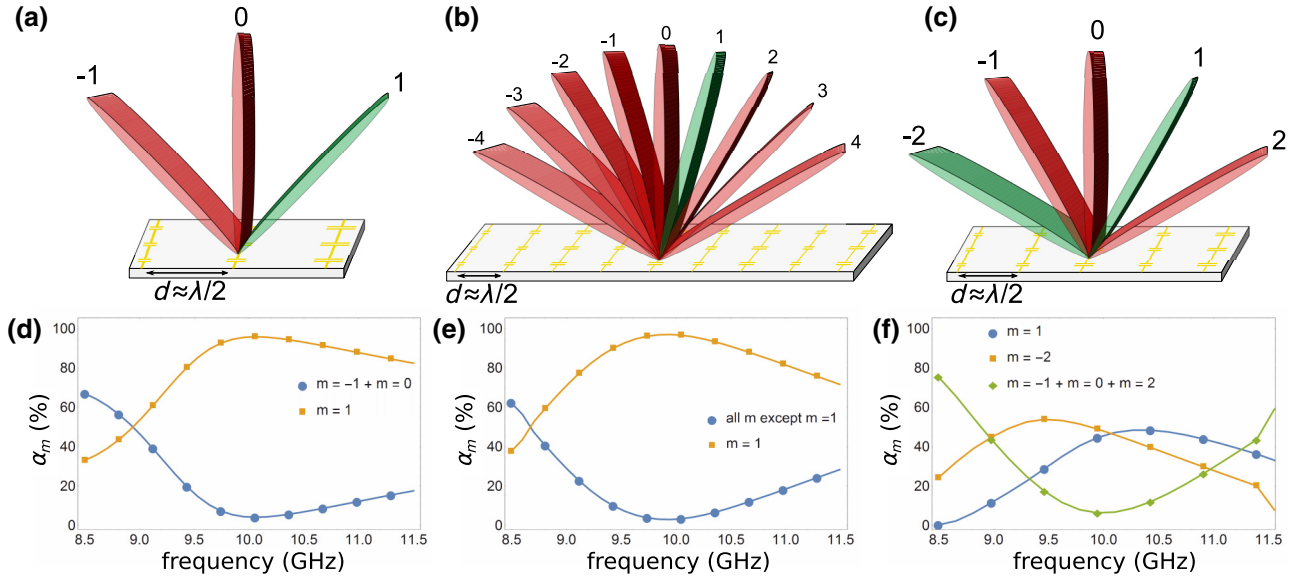

FIG. 3. The top row of figures demonstrates schematics of simulated metagratings with (a) $N = 3$, (b) $N = 9$, and (c) $N = 5$, the green and red lobes depict excited and canceled diffraction orders, respectively. The bottom row depicts 3D full-wave-simulation frequency responses of the metagratings corresponding to the figures in the top row. (a),(d) Anomalous reflection example at an angle of 50° with the metagrating having $N = 3$, $L = \lambda/\sin[50^\circ]$, and loads (in η/λ, $\tilde{\kappa} = 26.80$ mm) $Z_1 = -14.5j$, $Z_2 = -6.86j$, $Z_3 = -4.43j$. (b),(e) Small-angle anomalous reflection (of 12.5°) example with the metasurface having $N = 9$, $L = 4\lambda/\sin[60^\circ]$, and loads (in η/λ, $\tilde{\kappa} = 27.43$ mm) $Z_1 = -j\,7.62$, $Z_2 = -j\,6.96$, $Z_3 = -j\,6.19$, $Z_4 = -j\,5.55$, $Z_5 = -j\,5.18$, $Z_6 = -j\,3.57$, $Z_7 = -j\,3.02$, $Z_8 = -j\,18.7$, $Z_9 = -j\,10.1$. (c),(f) The example when out of five only −second and first diffraction orders are equally excited with the metagrating having $N = 5$, $L = 2\lambda/\sin[50^\circ]$, and loads (in η/λ, $\tilde{\kappa} = 27.18$ mm) $Z_1 = -9.00j$, $Z_2 = -5.88j$, $Z_3 = -6.59j$, $Z_4 = -3.03j$, $Z_5 = -5.14j$. The substrate is Arlon AD450 [$\varepsilon_s = 4.5$], $h = 3$ mm, $B = \lambda/10 = 3$ mm, and $w = 3$mil ≈ 76.2 μm.

orders and, therefore, only three polarization line currents per supercell are necessary to cancel the −first and zeroth diffraction orders, as illustrated in Fig. 3(a). Figure 3(d) depicts the frequency response of the metagrating performing anomalous reflection at an angle of 50°. The situation is more difficult in the case of a small-angle anomalous reflection with the presence of many high diffraction orders and when the energy should be scattered only in the first one. Indeed, in the example of Fig. 3(b) there are nine diffraction orders and the metagrating with nine polarization currents is used to cancel scattering in all of them except the first one corresponding to an anomalously reflected wave at an angle of 12.5°. Figure 3(e) demonstrates the frequency dependence of the metagrating's performance efficiency. Clearly, metagratings are not restricted to anomalous reflection application and can be used for multichannel reflection. One can distribute the energy of an incident wave between all diffraction orders in a desirable manner. For instance, Figs. 3(c) and 3(f) demonstrate the scenario when the metagrating having five polarization currents is used to split normally incident waves between the −second and first diffraction orders and cancel scattering in the other three diffraction orders.

In conclusion, it has been shown that a metagrating having the number of polarization line currents per supercell equal to the number of plane waves scattered in the far field can be used for controlling the diffraction pattern. Namely, Eqs. (3) and (4) allowing one to find currents realizing desirable transformations have been derived. Since there are no analytical formulas of reactive load-impedance densities (5) for direct design, genetic algorithms have been implemented for that purpose. The diffraction-order control has been demonstrated by means of 3D full-wave simulations on the examples of anomalous reflection and equal redistribution of the energy of the incident wave between two diffraction orders.

The validation results are very interesting for the metamaterials community to perform highly efficient control of light scattering. It allows one to significantly decrease the number of used elements and simplify the design, which is very convenient for optical and infrared frequency ranges. Our findings may also provide a way to develop efficient tunable antennas in the microwave domain.

[1] S. V. Hum, M. Okoniewski, and R. J. Davies, Realizing an electronically tunable reflectarray using varactor diode-tuned elements, IEEE Microw. Wirel. Compon. Lett. **15**, 422 (2005).

[2] S. V. Hum, M. Okoniewski, and R. J. Davies, Modeling and design of electronically tunable reflectarrays, IEEE Trans. Antennas Propag. **55**, 2200 (2007).

[3] Nanfang Yu, Patrice Genevet, Mikhail A. Kats, Francesco Aieta, Jean-Philippe Tetienne, Federico Capasso, and Zeno Gaburro, Light propagation with phase discontinuities: Generalized laws of reflection and refraction, Science **334**, 333 (2011).

[4] Stanislav B. Glybovski, Sergei A. Tretyakov, Pavel A. Belov, Yuri S. Kivshar, and Constantin R. Simovski, Metasurfaces: From microwaves to visible, Phys. Rep. **634**, 1 (2016).

[5] V. S. Asadchy, M. Albooyeh, S. N. Tcvetkova, A. Díaz-Rubio, Y. Ra'di, and S. A. Tretyakov, Perfect control of reflection and refraction using spatially dispersive metasurfaces, Phys. Rev. B **94**, 075142 (2016).

[6] Carl Pfeiffer and Anthony Grbic, Metamaterial Huygens' Surfaces: Tailoring Wave Fronts with Reflectionless Sheets, Phys. Rev. Lett. **110**, 1 (2013).

[7] V. S. Asadchy, A. Díaz-Rubio, S. N. Tcvetkova, D.-H. Kwon, A. Elsakka, M. Albooyeh, and S. A. Tretyakov, Flat Engineered Multichannel Reflectors, Phys. Rev. X **7**, 031046 (2017).

[8] Ana Díaz-Rubio, Viktar S. Asadchy, Amr Elsakka, and Sergei A. Tretyakov, From the generalized reflection law to the realization of perfect anomalous reflectors, Sci. Adv. **3**, e1602714 (2017).

[9] Ariel Epstein and George V. Eleftheriades, Synthesis of Passive Lossless Metasurfaces using Auxiliary Fields for Reflectionless Beam Splitting and Perfect Reflection, Phys. Rev. Lett. **117**, 256103 (2016).

[10] Badreddine Ratni, André de Lustrac, Gérard-Pascal Piau, and Shah Nawaz Burokur, Reconfigurable meta-mirror for wavefronts control: Applications to microwave antennas, Opt. Express **26**, 2613 (2018).

[11] Younes Ra'di, Dimitrios L. Sounas, and Andrea Alù, Metagratings: Beyond the Limits of Graded Metasurfaces for Wave Front Control, Phys. Rev. Lett. **119**, 067404 (2017).

[12] Ariel Epstein and Oshri Rabinovich, Unveiling the Properties of Metagratings via a Detailed Analytical Model for Synthesis and Analysis, Phys. Rev. Applied **8**, 054037 (2017).

[13] O. Rabinovich and A. Epstein, Analytical design of printed-circuit-board (pcb) metagratings for perfect anomalous reflection, IEEE Trans. Antennas Propag. 1 (2018).

[14] Alex M. H. Wong and George V. Eleftheriades, Perfect Anomalous Reflection with a Bipartite Huygens' Metasurface, Phys. Rev. X **8**, 011036 (2018).

[15] H. Chalabi, Y. Ra'di, D. L. Sounas, and A. Alù, Efficient anomalous reflection through near-field interactions in metasurfaces, Phys. Rev. B **96**, 075432 (2017).

[16] Younes Ra'di and Andrea Alù, Reconfigurable metagratings, ACS Photonics **5**, 1779 (2018).

[17] L. B. Felsen and N. Marcuvitz, *Radiation and Scattering of Waves* (IEEE Press, New York, 1994).

[18] Sergei Tretyakov, *Analytical Modeling in Applied Electromagnetics* (Artech House, Norwood, MA, 2003).

[19] See Supplemental Material at http://link.aps.org/supplemental/10.1103/PhysRevApplied.0.xxx for the derivation of formulas (2) and (5) presented in the main text.

[20] Alden H. Wright, *Genetic Algorithms for Real Parameter Optimization* (Elsevier, San Mateo, 1991) pp. 205–218.